Magnetic Field cartography of the Hall A ^{3}He Polarized Target

Alexandre Deur, deurpam@cebaf.gov, Jian-Ping Chen, jpchen@cebaf.gov

06/26/1998

Abstract

The Hall A Helium 3 Polarized Target, currently built at Jefferson Lab, is a 10 Atm, 40 cm length target filled of Helium. In order to align the spin of the ^{3}He nuclei and to perform NMR/EPR polarimetry the target is surrounded by two pairs of Helmholtz coils. The good homogeneity of the field (gradients inferior to 20 mGauss/cm) is important for a long cell polarization life time (several hundreds of hours). It is also critical to not destroy the target polarization during the NMR magnetic field sweeps. A first field mapping to check if the field gradients were tolerable was performed. An upper limit of these gradients was delivered and found acceptable. Another goal was to check the consistency of the field with the coils setup (i.e. to check if the coils are well built and accurately aligned). A second mapping was done with a more precise setup to give an accurate value of the gradients in order to check the coil alignment. This note presents the description of the experimental setup and the result of the mapping.

1 Introduction

The homogeneity of the main magnetic field in the Polarized ^{3}He Target plays an important role.

- The field gradient has an impact on the polarization lifetime: inhomogeneities are view, from the moving ^{3}He gas frame, as time dependant fields that can induce nuclear transitions implying a loss of polarization [1], [2]. The characteristic (relaxation) time is given for the Helmholtz coils aligned on the z-axis by: $\frac{1}{\tau_{\nabla B}} = D\frac{|\nabla B_x|^2+|\nabla B_y|^2}{B_z^2}$ where ∇B_x and ∇B_y are the inhomogeneities of the field transverse to the alignment field B_z. D is called the self-diffusion constant. D=0.244 cm^2.s^{-1}. A typical value of B_z is 34 Gauss. With gradients lower than 20 mG.cm^{-1} the lifetime is greater than 500 hours. That is long enough in comparison with the other depolarisation processes.

- Inhomogeneous fields decrease the transverse relaxation time T_2' of the ^{3}He to $T_2'^*$[3]: $\frac{1}{T_2'^*} = \frac{1}{T_2'} + \frac{1}{T_2^g}$ where $T_2^g = \gamma \nabla B$ with γ the gyromagnetic ratio of the proton. This implies a larger width of signal and a smaller high (see Bloch equations). This effect can be understood as following. The magnetic field is swept to perform the NMR polarimetry by Adiabatic Fast Passage. The inhomogeneities will make all the nuclear spins to not flip at the same time. The result is that a such polarization measurement will increase the signal width and decrease the magnitude.

- To check if the field shape is understood as well as it's magnitude.

- To check if some devices near the coils are not creating high disastrous gradients.

- To provide a way to align the coils in order to minimize the field gradients coming from some main coils misalignment.

2 First mapping

The mapping was done three times. The was done in the FEL building in order to check if the gradients were small enough. The frame of the target was a temporary wooden frame. The second and third mappings were done in the EEL building to see if the new target metallic frame (mostly in aluminium) and the new setup in the Target Lab did not induce new gradients. As no survey of the target dimensions was done in the FEL we are not able to compare the EEL data with the EEL data.

2.1 Experimental Setup

2.1.1 Magnetic Probes

Two devices were used to measure the field. A Hall probe[1] that can measure the magnetic field magnitude actually used to run the target (around 34 Gauss). The drawback being the 10 mGauss precision on the measurement. Nevertheless this is sufficient to check if the gradients are tolerable. A 10 A current for the Helmholtz coils is provided by a Kepco BOP 36-12D power supply[2]. Although it is used in voltage mode during target operations, we used it in current mode to have a stable magnetic field: due to Joule Effect the resistance of the coils drift and a voltage mode will automatically adjust the current to keep the setting value of the voltage, inducing a drift in the field. The magnitude of the large component of the field is 34.2 Gauss for 10 A.

[1]Provided By J. J. Lerose, Jefferson Lab.

[2]The actual current in the coils is slightly higher than the KEPCO front panel indications (10.16 A instead of 10 A).

A second device was used (Magnetoscop 1.068, Institute Dr Forster[3]). It is more precise but can handle only a 1 Gauss magnitude field. This is not a problem if we assume the gradients are, as the field, linear with the coil current (that is there are no heavy magnetic objects near the coils). This problem does not appear during the measurement of the small (transverse) field components. For the large component measurements the coil current was set at 0.25 A (i.e around 0.88 Gauss). The Magnetoscop could be used in two modes: Magnitude measurements and gradient measurements. As the second mode was found not accurate enough, only the first one was used. The probe is made by two coils of 3 cm length, spaced out by 2 cm and so measures the average field on a 3×2 cm^2 area.

2.1.2 Axis Definition and Reference Point

The axis are defined in the figure below.

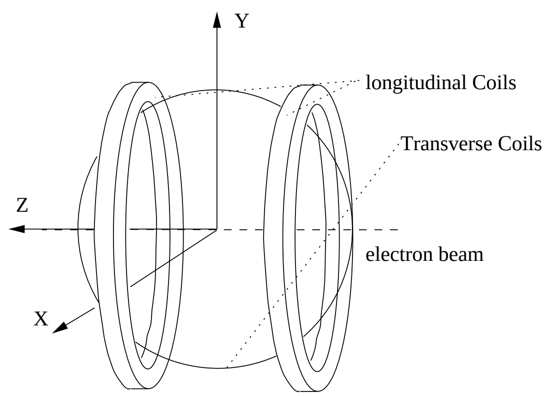

Fig.1 Axis definition.

A reference point (x=0, y=0, z=0) was chosen close to the geometrical center of the coils: the center on the horizontal plan is defined by the intersection of the two lines going through the centers of the four screw holes surrounding the central hole (see figure 2). The high of the center was determined using marks on the mid high of the transverse coils. These marks were placed during the first geometrical survey of the target[4] (fig. 2).

[3] Provided by Z.E Meziani, Temple University.

[4] Incidentaly the first survey has shown that one of the longitudinal coil was bent. we can see the effect on the second plot of fig. 7 page 8.

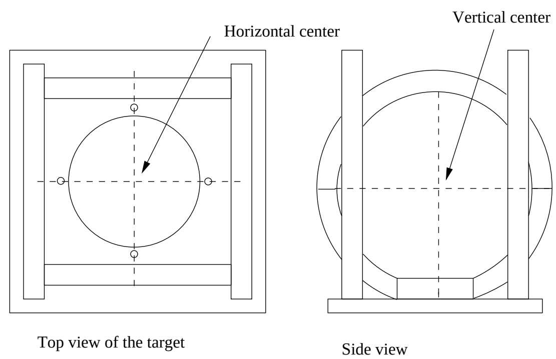

Fig. 2 Reference Point.

2.1.3 Inclinometer

The Hall probe is very sensitive to its inclination. If the probe is tilted with θ instead of measuring the field B_m we will measure $B_m cos\theta + B_t sin\theta$ where B_t is the field component transverse to B_m. If B_m is a small component of the magnetic field then B_t is of order of 34 Gauss and a value of $\theta = 3 \times 10^{-4}$ radian adds a false field gradient of 10 mGauss to the actual gradient. This shows the necessity of an inclinometer to record the relative angle θ from point to point.

I have used an inclinometer provided by P. Vernin. It is made of a capacitor containing a mercury droplet resting on a curved plate. On horizontal position the droplet is in the center of the capacitor. If the inclinometer is a little tilted the droplet moves closer to one of the capacitor edges, changing the capacity. A DC voltage source and a multimeter allow a measurement of the capacitor voltage. Using Johnson wedges we have calibrated the device. Defining the angle as in fig. 3 (thanks to the CG10 label) we found the relation: $\Delta V \equiv -0.5$ mRad.

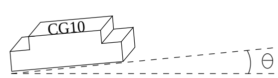

Fig. 3 angle definition.

2.2 Computation

To compare the measures to some computed results one has used two codes (Location: ˜deurpam/RMN/). The first, written by G. Quemener, simulates the coils as two helicoids. Every loop was made of 100 segments. The second code computes the field by numerical integration of the Biot and Savart law. Each segment has a length of about 3 cm. The integration converges (i.e. with differences in results inferior to 0.01 mGauss) for integration steps of 3 mm.

The code was checked in the simple case of only one loop with the field direction along the axis of the loop. The analytic solution in this particular case is $B = \frac{\mu_0 I}{2R}$ where μ_0 is the vacuum magnetic permeability, I the current in the loop and R the loop radius. The analytical result and numerical result agree within 0.02 mGauss.

The current was read on the Kepco display with a 0.01 A precision. That is acceptable for 10 A mapping. For the 0.25 A operations we have a 4% error on the field. That explains the error bars on the computation results.

2.2.1 How to use the computation codes ?

The first step is to get a coil model by running helice.f for the longitudinal coils and helice_t.f for the transverse coils. The table below gives the parameters for the two codes.

coils	ncouche	nspire	rayon (mm)	pas_helice	pas_rayon	centre(3,1)	centre(3,2)
transverse	16	16	633.41	4.266	3.987	304.8	-373.06
longitudinal	16	17	723.90	4.669	4.266	346.07	-425.45

ncouche is the number of layers while nspire is the number of loops

rayon is the coil internal radius, pas_helice is the distance between two loops while pas_rayon is the distance between two layers.

centre(3,1) is the z-position of the internal loop center of one coil.

centre(3,2) is the z-position of the external loop center of the other coil (see fig 4).

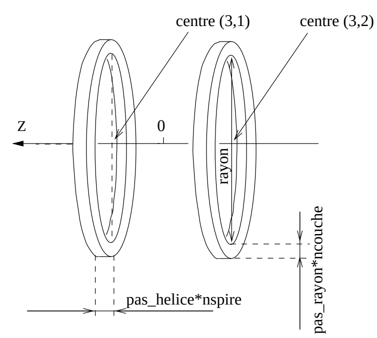

Fig. 4 parameters definition used in the computation codes.

The coil model data are stored in the file seg.dat.

The second step is to run champ2.f. The inputs are the offset positions from the reference point and the direction of the probe movement. It stores the data for the magnetic field components x,y and z in respectively champx.dat, champy.dat and champz.dat. One did not make another code for the transverse coils so one has to run the same code and to substitute x to z, z to x and y to -y.

Note. For the two first mappings the coils were misaligned and not flat. This gradient source was simulated in the computation (see comment of fig. 6).

2.3 Errors estimation

A first error comes from the Magnetoscop dial reading and from the device class: $\Delta B = \pm 2.5\%$ of the maximum range value $+\frac{1}{4}$ graduation. For the Hall probe the error is on the last digit that is $\Delta B = \pm 10$ mGauss.

The maximum error on the inclinometer is the error on the last digit of the multimeter time the calibration time the highest field expected. One has $\Delta B = 2 \times 10^{-2}$ mGauss that is we can neglect it.

One has also to give an upper estimation on the error arising from the fact that the probe displacement is not perfectly parallel to the sweeping axis i, say by an angle α. If j is the other axis in the horizontal plan we have $B_i = B_i^{measured} + \frac{\partial B_j}{\partial j}|_0 \times step \times sin\alpha$. We have, according to the field computation and the measurements: $\frac{\partial B_j}{\partial j}|_0 < 10$ mGauss/cm, $step = 1$ cm and a large value for α is $\alpha = 0.01$ rad. This provides an upper value less than 2 mGauss.

We will assume a ± 1 mm error on the relative position of the probe.

2.4 Offsets

Due to uncertainty on the actual current (cf footnote page 2) we have an unknown offset on the measuring field. Another unknown offset comes from the fact that the rail where the probe is sliding can be tilted. The inclinometer, measuring only relative tilts, is useless in this case.

An arbitrary offset is added to the computation result to match the data. That is the computation will check accurately the field shape and roughly its magnitude. An earth field correction is not relevant since it adds a constant offset that is already included in the arbitrary added to the data

2.5 Results

Three mappings were performed. The first one in the FEL building, the two others in the EEL building. The figures below present the results of the second mapping. As we first did the FEL mapping in voltage mode we had to correct the results from the current drift. Also we did not use inclinometer and reference point. We have plotted only EEL data since we cannot compare FEL and EEL data. FEL and computed data cannot also be compare since we did not have a coils survey for the FEL mapping. The result of the FEL mapping gave reasonable upper limit of the gradients and consequently a polarization lifetime long enough. The lower limit was 650 hours.

The more accurate EEL data are plotted below.

2.5.1 Scaterring chamber level

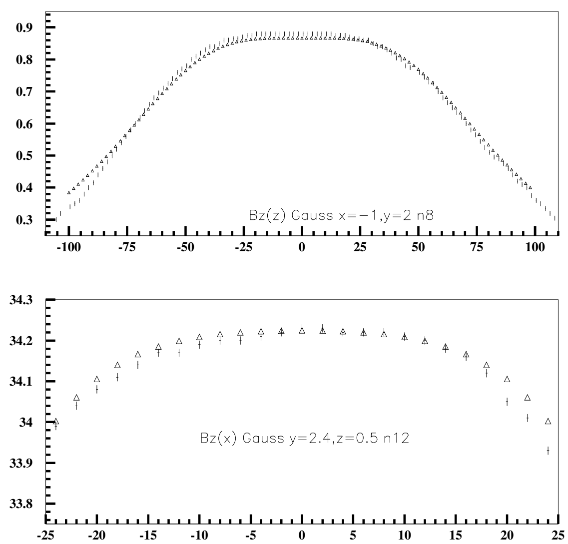

Fig.5 z-components of the field for the longitudinal coils at I=0.25 A for the first plot and I=10.16 A for the second. The dots are the experimental results while the triangles are the model. The error bars on the computation results are to small to be seen. The position offsets are in meter and were added to the model. We use the Magnetoscop for the first plot. Since the direction of the field is along the probe detection coils we do not need inclinometer correction. For the second plot we used the Hall probe. The variation of the inclination was around 0.05 mRad and the magnitude of the transverse field component (following the model) 10^{-2} *Gauss. That is the inclination correction is less than 0.25 mGauss and can be neglected.*

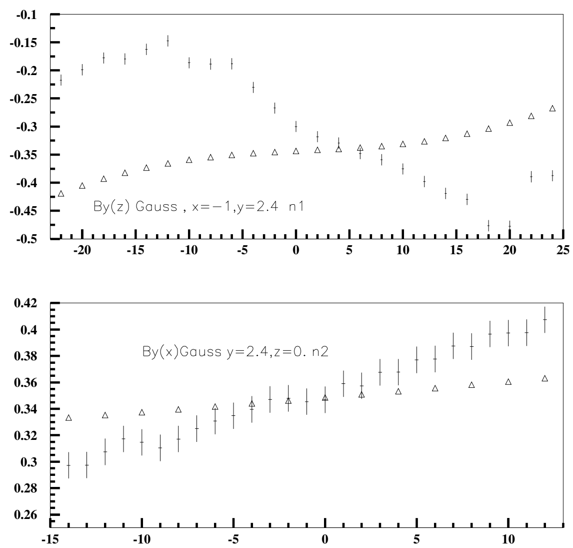

Fig.6 y-components of the field for the longitudinal coils at I=10.16 A. The dots are the experimental results while the triangles are the model. We used the Hall probe for the two plots. Similar computation that we have done for fig. 4 shows both plots had needed inclinometer correction (The correction can reach 1. mGauss). We have simulate a non flatness of the coil in bending one quarter of the coil 2 (i.e. the coil of negative z-coordinates) by 8 mm. However it did not explain all the discrepancy between the model and the measurement. A coil bent by -40 mm fits very well the measurements but this was not seen during the geometrical survey. The figure 17 results are consistent with the fact that these gradients come from a coil misalignment.

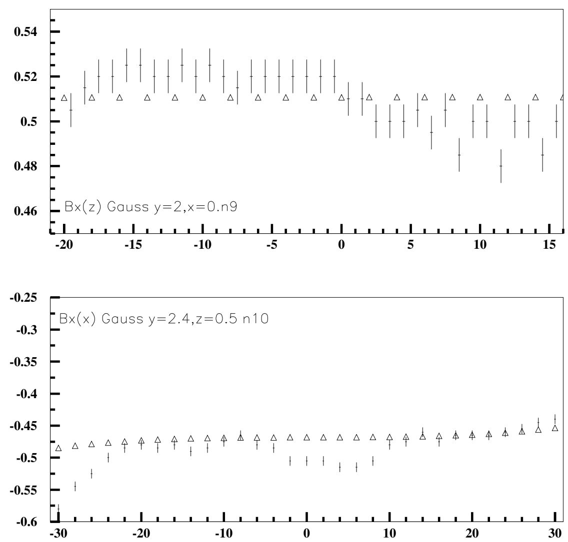

Fig.7 x-components of the field for the longitudinal coils at I=10.16 A. The dots are the experimental results while the triangles are the model. We used the Magnetoscop for the two plots and thus did not need inclinometer correction. One can explain the experimental shape of the first plot (looking like the one of the second plot) by the fact that the probe displacement was not perfectly perpendicular to the coils and thus gives a mixing of the z and x components. This is consistent with the fact that the experimental shape of the second plot is less marked than the computation shape.This shape comes from the fact that the distance between the two coils is not exactly the radius of the coils (for perfect Helmholtz coils it should be flat). The bigger slope one the left side shows the coil is bent (see footnote p3).

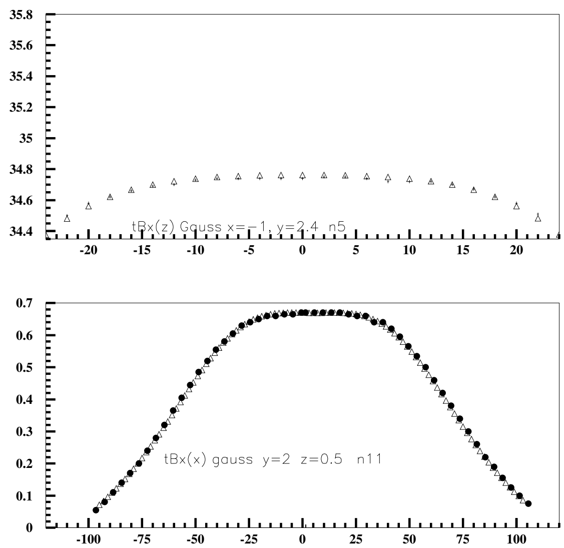

Fig.8 x-components of the field for the transverse coils at I=10.16 A for the first plot and 0.25 A for the second plot. The dots are the experimental results while the triangles are the model. We used the Hall probe for the first plot and Magnetoscop for second. We did not need inclinometer correction (as in fig. 5).

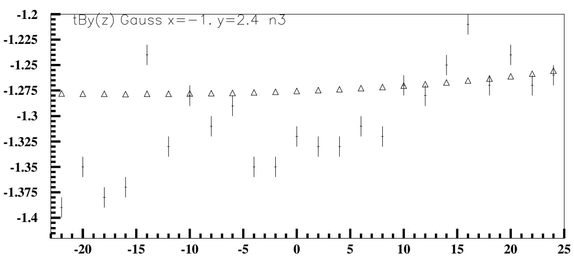

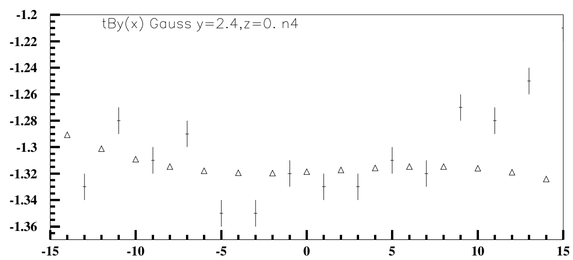

Fig.9 y-components of the field for the transverse coils at I=10.16 A. The dots are the experimental results while the triangles are the model. We used the Hall probe for both plots and need inclinometer correction (not done).

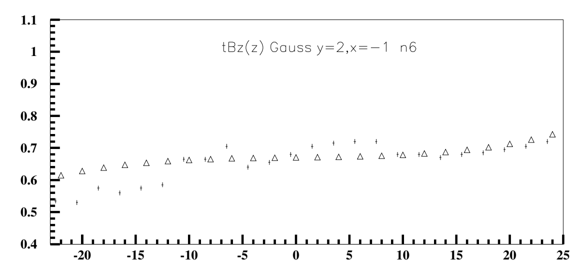

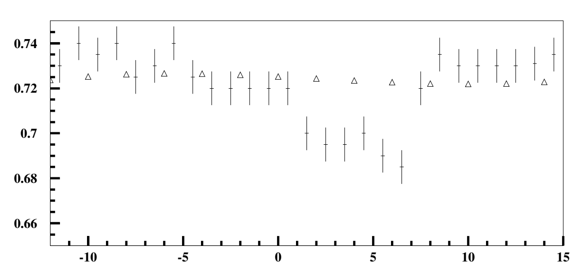

Fig.10 z-components of the field for the transverse coils at I=10.16 A. The dots are the experimental results while the triangles are the model. We used the Magnetoscop for both plots and thus did not need inclinometer correction.

2.5.2 Pumping chamber level

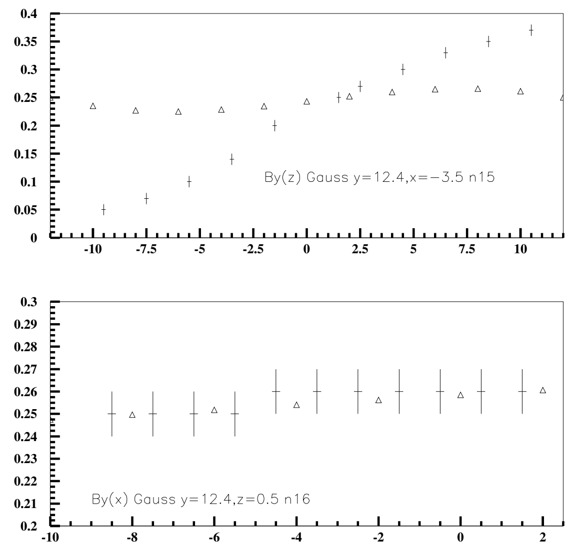

Fig.11 x-components of the field for the longitudinal coils at I=10.16 A. The dots are the experimental results while the triangles are the model. We used the Hall probe for both plots. As in Fig. 6 we have corrected the non-flatness of a coil but 8 mm is not enough to explain the first plot shape .

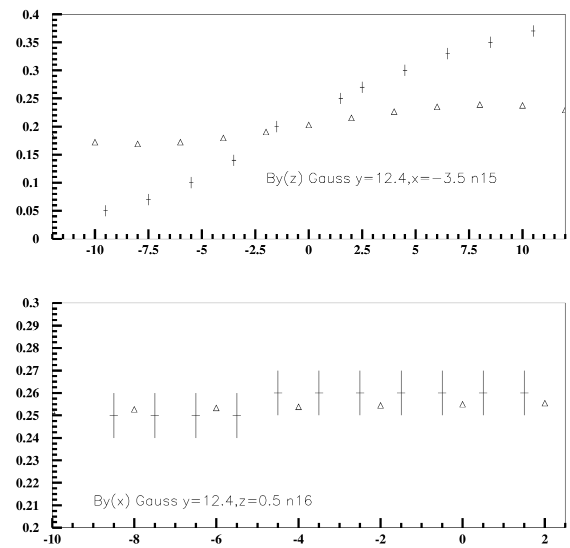

Fig.12 y-components of the field for the longitudinal coils at I=10.16 A. The dots are the experimental results while the triangles are the model. We used the Hall probe for both plots.

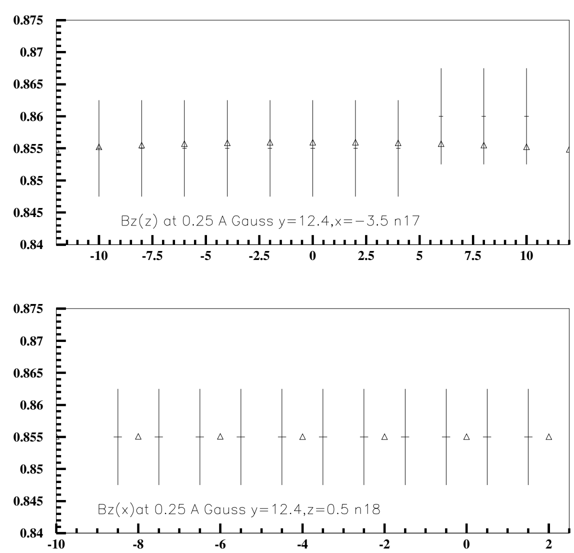

Fig.13 z-components of the field for the longitudinal coils at I=10.16 A. The dots are the experimental results while the triangles are the model. We used the Magnetoscop for both plots.

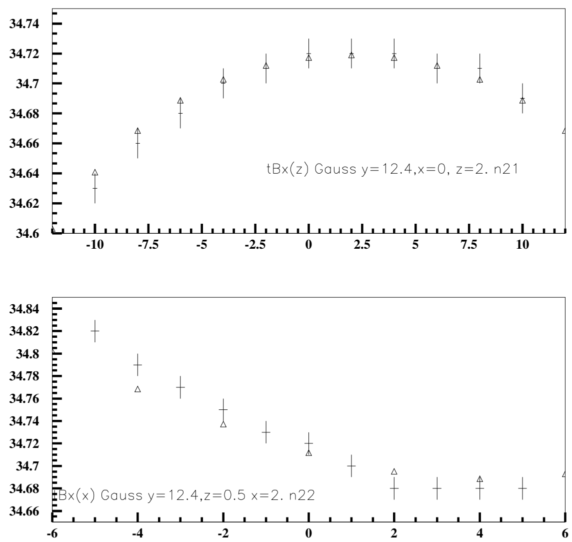

Fig.14 x-components of the field for the transverse coils at I=10.16 A. The dots are the experimental results while the triangles are the model. We used the Hall probe for both plots.

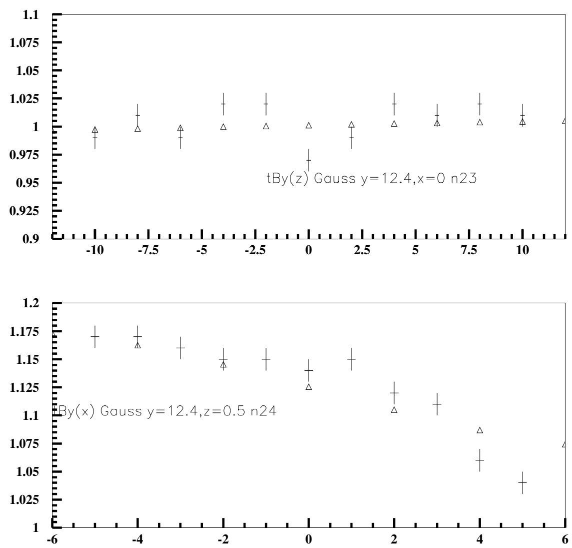

Fig.15 y-components of the field for the transverse coils at I=10.16 A. The dots are the experimental results while the triangles are the model. We used the Hall probe for both plots.

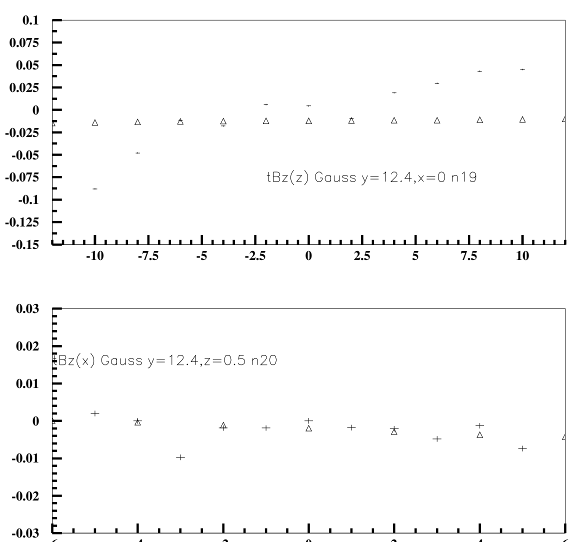

Fig.16 z-components of the field for the transverse coils at I=10.16 A. The dots are the experimental results while the triangles are the model. We used the Magnetoscop for both plots.

2.6 Conclusions

The main conclusion of the second mapping is that all the gradients, within the cell area, excepting for two cases, are less than 20 mGauss. That yields long enough polarization lifetime (see paragrapher 4).

Changing the model parameters shows important dependence of the field shape with the offsets.

The computation results and data for transverse coils agree well. We have to investigate that one longitudinal coil was bent.

3 Third mapping

A second mapping was done in the EEL building after a second geometrical survey and the set up of the definitive target top. It was done in order to check if the gradients stayed tolerable after the addition of the new top. We checked only some of the field components, in particular these providing gradients due to some misalignments of the coils. The second survey allowed to align the coils more precisely.

3.1 Results

The figure 17 presents the results of this cross-checking mapping. The measurements are compared with the previous ones. The simulated results are the same than previously.

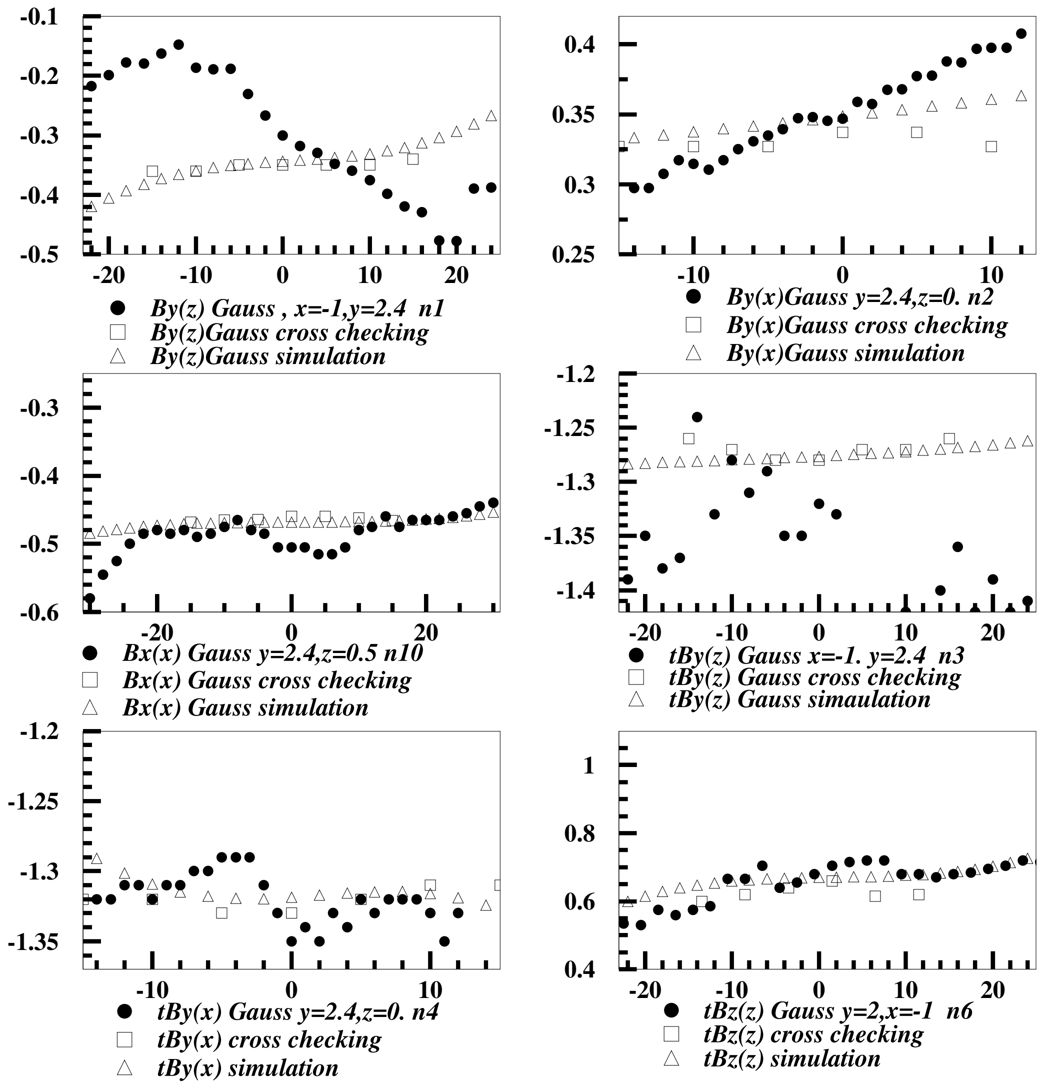

Fig. 17 Second measurements for the target with its definitive top (squares). The circles and triangles are the previous results plotted for comparison.

The gradients are smaller than the previous ones which is consistent with the assumption that the gradients of fig. 6, 11, 12 and 16 were due to misalignments. We also used a new mapping setup that allowed more precision and less inclination errors.

4 Polarization lifetime

4.1 Computation

The mapping allows the computation of the polarization lifetime (not taking into account the other phenomena that will reduce the lifetime). Since we have not mapped in the vertical direction (i.e. y) we use homogeneous Maxwell equations to deduce the vertical field gradient:

$\vec{\nabla} \wedge \vec{B} = 0$ that implies $\frac{\partial B_x}{\partial y} = \frac{\partial B_y}{\partial x}$ and $\frac{\partial Bz}{\partial y} = \frac{\partial B_y}{\partial z}$.

$\vec{\nabla}\vec{B} = 0$ that is $(\frac{\partial B_y}{\partial y})^2 = (\frac{\partial B_x}{\partial x} + \frac{\partial B_z}{\partial z})^2$

The table below gives the gradients (Gauss/cm) for the two target chambers levels and the two Helmholtz coils sets. The gradients were computed from the second mapping data.

gradient	$\frac{\partial B_x}{\partial x}$	$\frac{\partial B_x}{\partial y}$	$\frac{\partial B_x}{\partial z}$	∇B_x^2	$\frac{\partial B_y}{\partial x}$	$\frac{\partial B_y}{\partial y}$	$\frac{\partial B_y}{\partial z}$	∇B_y^2	$\frac{\partial B_z}{\partial x}$	$\frac{\partial B_z}{\partial y}$	$\frac{\partial B_z}{\partial z}$	∇B_z^2
Long, scat	2	4	4	36	4	5	16	297	2	16	5	285
Long, pump	5	5	5	75	5	7	20	474	0	20	5	425
Trans, scat	2	5	2	33	5	4	10	141	10	10	4	216
Trans, pump	8	25	5	714	25	9	5	731	0	5	3	34

We deduce the lifetime for the scattering chamber under the longitudinal field:

$\tau_{\triangle B} = (D\frac{|\nabla B_x|^2+|\nabla B_y|^2}{B_z^2})^{-1}$=1.422×10^7 s = 3950 hours

The lifetime for the pumping chamber under the longitudinal field:

$\tau_{\triangle B} = (D\frac{|\nabla B_x|^2+|\nabla B_y|^2}{B_z^2})^{-1}$=8.689×10^6 s = 2414 hours

The lifetime for the scattering chamber under the transverse field:

$\tau_{\triangle B} = (D\frac{|\nabla B_z|^2+|\nabla B_y|^2}{B_x^2})^{-1}$=1.327×10^7 s = 3686 hours

The lifetime for the pumping chamber under the transverse field:

$\tau_{\triangle B} = (D\frac{|\nabla B_z|^2+|\nabla B_y|^2}{B_x^2})^{-1}$=6.189×10^6 s = 1719 hours.

4.2 Conclusion

This lower limit is high enough to not be concerned by the gradient relaxation process. With the new top and new survey the lifetime is higher.

5 Inputs sensibility of the model

In order to know what uncertainty we can tolerate on the coil position we have investigated the sensibility of the computation with the geometric inputs of the coils models. These inputs were:

- the inner interface distance of the coils

- the flatness of the coils. The parameter being the shift on the position of the coil top. According to the survey one quarter of the coil was bent in the positive z-direction by 8 mm.

- inclination of the coils (the faces remaining parallele). The parameter is the maximum difference between the inclined coils and perfect positioned coils.

- bad parallelism of the coil. The parameter is the maximum distance between the inner faces. The center is unchanged.

5.1 Results

The four figures below give the computation for perfect coils (circles) and the computation after the variation of one parameter (squares). All the computations were done with 10 A current in each coils.

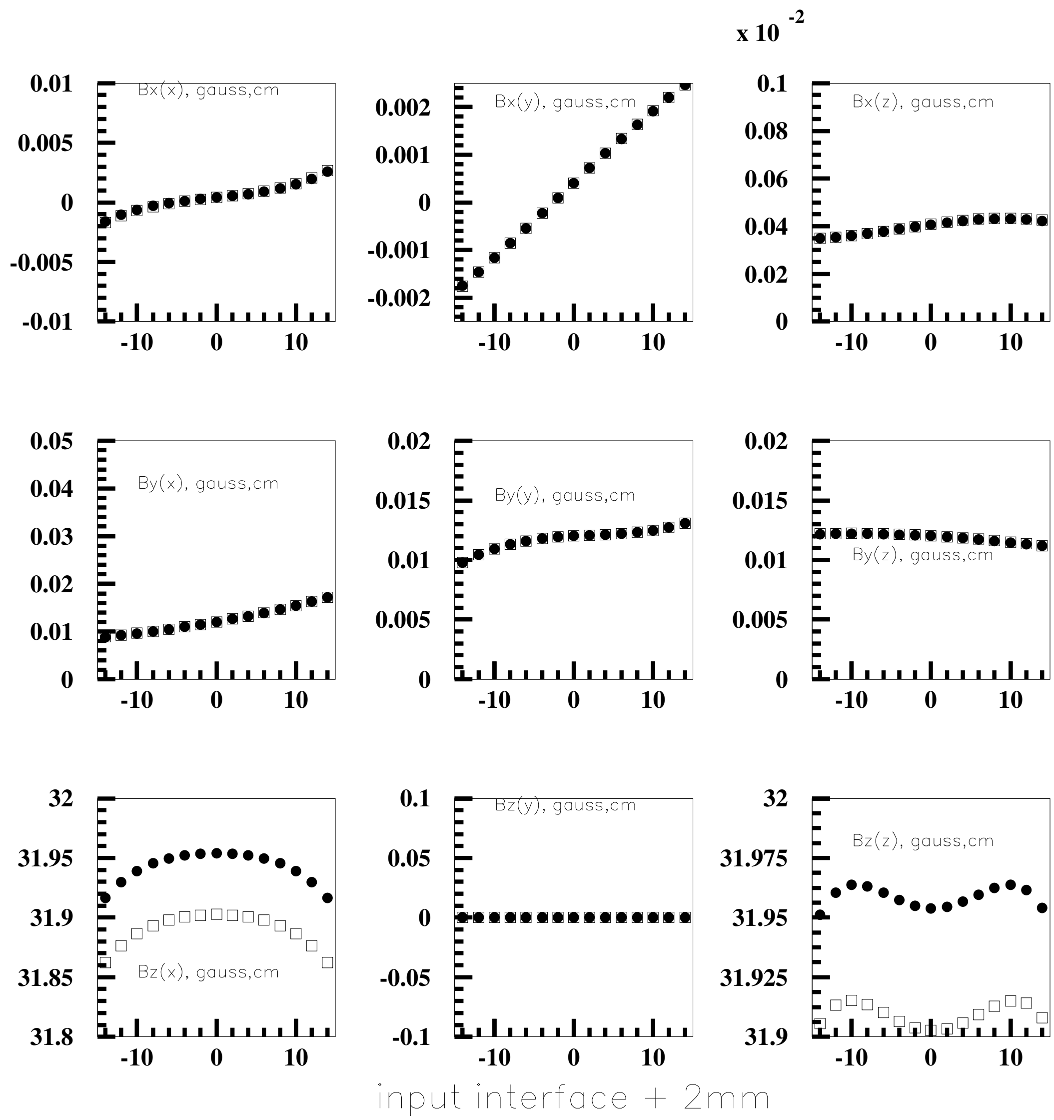

Fig. 18 The interface distance is increased by 2 mm (squares). The $B_z(z)$ gradient is increase from 0.83 mGauss/cm to 1.6 mGauss/cm. The increase of the $B_z(x)$ gradient is not important since it does not occur in the target area.

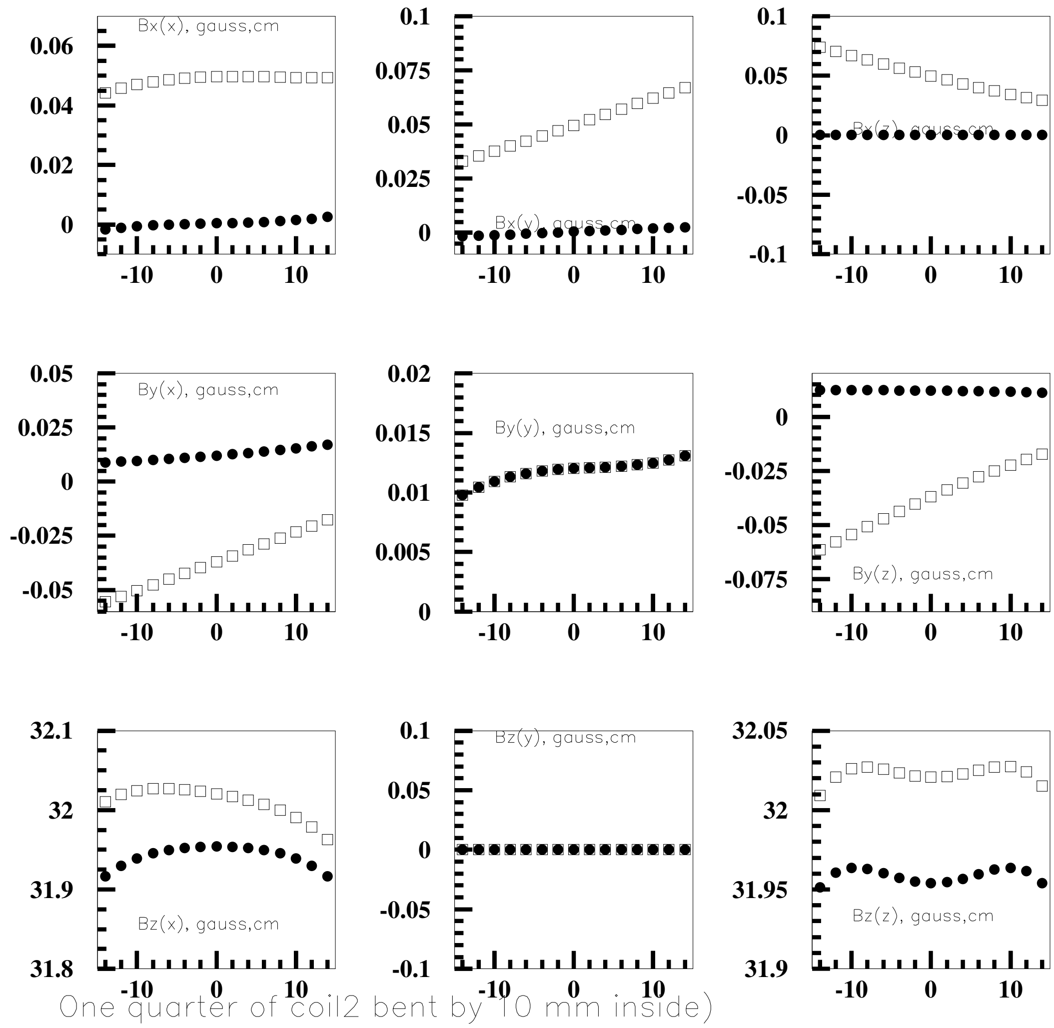

Fig. 19 The gradients due to a 10 mm non flatness of the coils are 1.3 mGauss/cm for $B_x(y)$, 2 mGauss/cm for $B_x(z)$, 1 mGauss/cm for $B_y(x)$, 1.6 mGauss/cm for $B_y(z)$ and 1 mGauss/cm for $Bz(x)$.

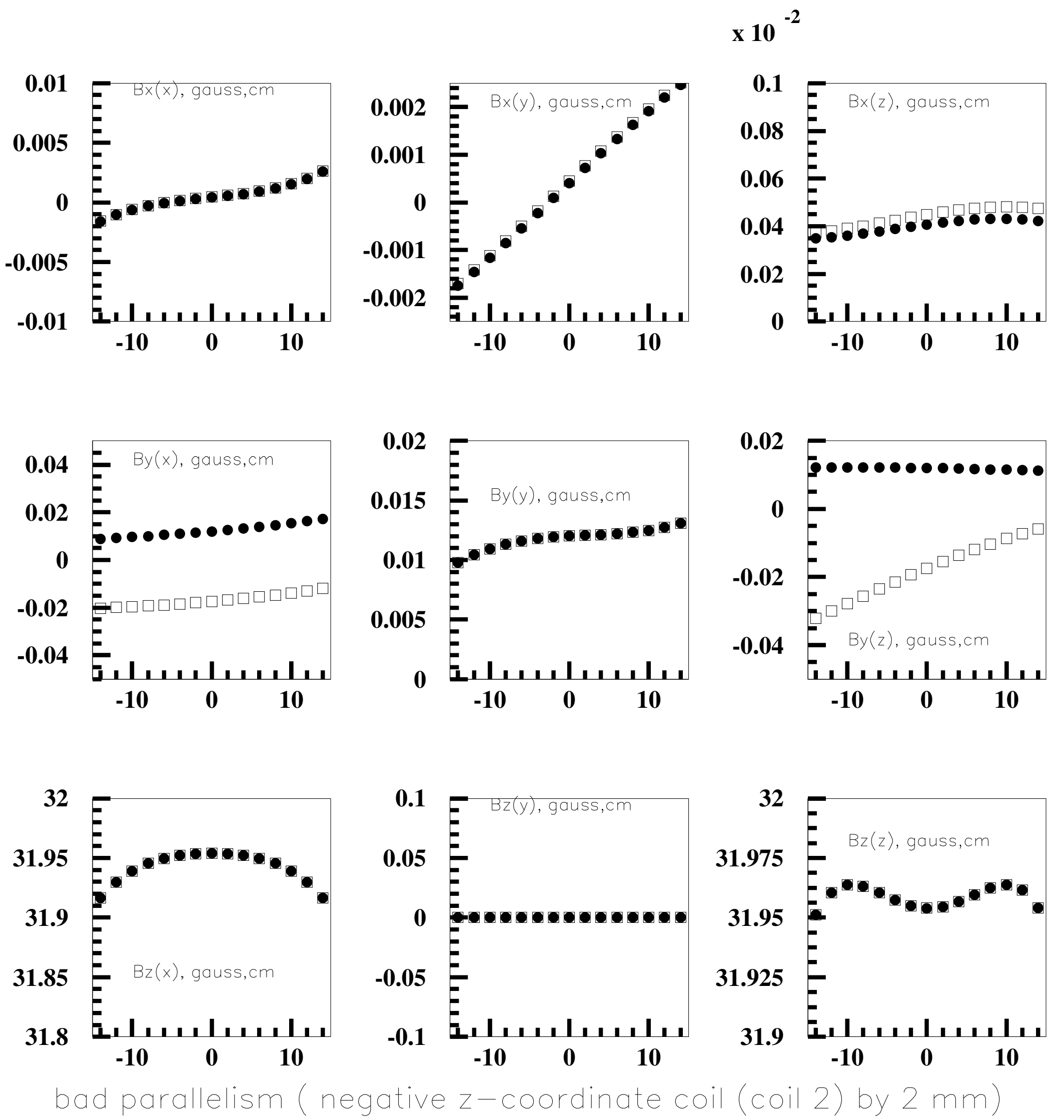

Fig.20 The maximum deviation from to perfectly coils is 2 mm. The effect of such non-parallelism is to give rise of a $B_y(z)$ gradient of 1.1 mGauss.

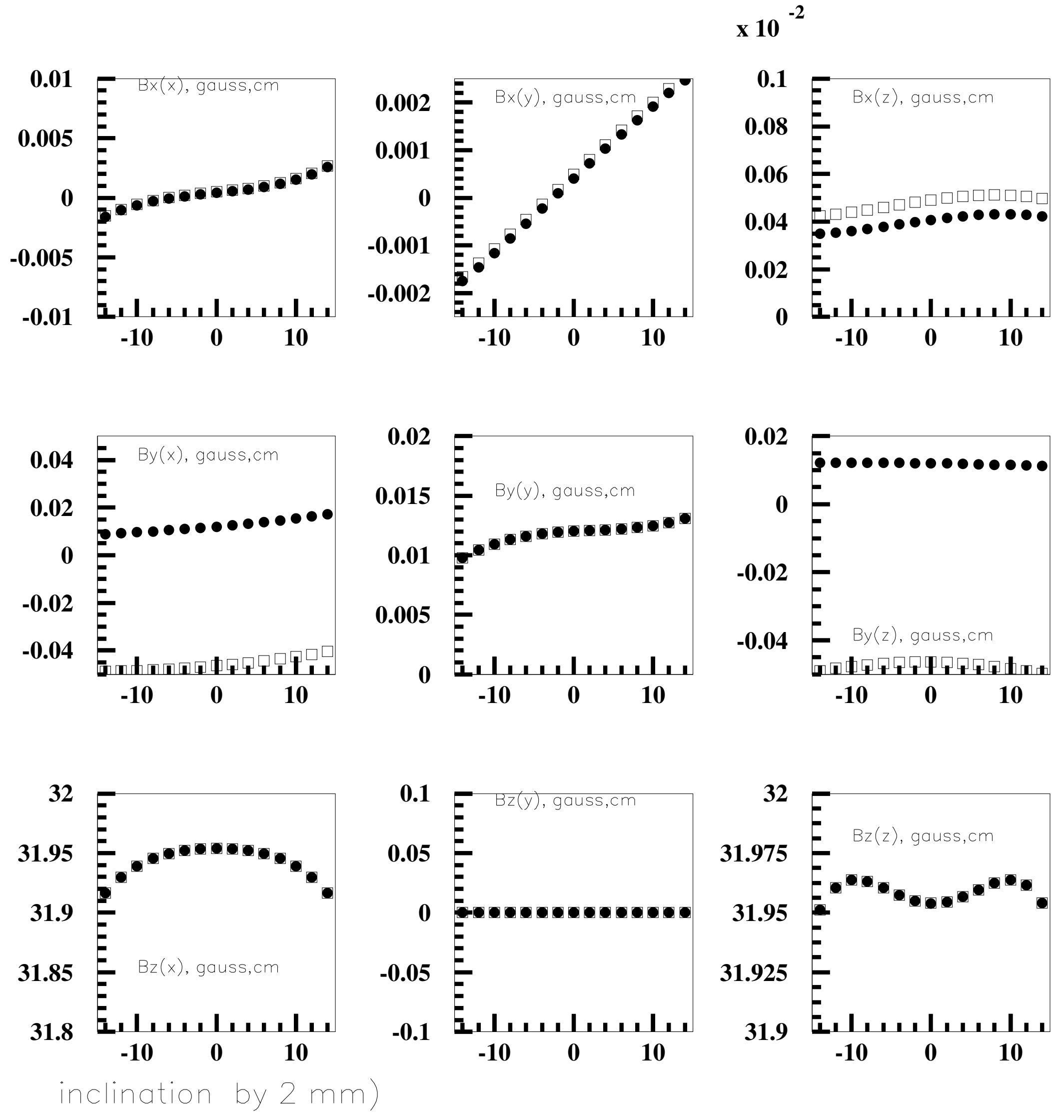

Fig.21 The inclination of both coil does not create or increase the value of the gradients but for By(z) *where the gradients are below 0.2 mGauss/cm.*

5.2 Conclusion

The computations above shows an uncertainty of ±1 mm does not increase the gradients by much than 3 mGauss/cm. However one should be aware that the results give minimum values since we have not compute the effect of several misalignments taken together. We have also assumed that the target will be in the geometrical center of the Helmholtz coils and thus have not added offsets on the computation parameters. The effect of offsets can be seen anyway since all the components of the field swept in the three directions are plotted.

Acknowledgements. We want to thank G. Quemener and P. Vernin for their advises and great help.

References

[1] E.W Hughes. Proc 21^{st} annual SLAC summer institute on Particle Physics. Spin structure in High Energy Processes (SLAC, Stanford 1993).

[2] H.L Middleton phD. thesis Princeton University (1994)

[3] Abragam. The Principle of Nuclear Magnetism. Oxford University Press 1961.